

## Investigation of isospin-triplet and isospin-singlet pairing in the $A = 10$ nuclei $^{10}\text{B}$ , $^{10}\text{Be}$ , and $^{10}\text{C}$ with an extension of the Tohsaki-Horiuchi-Schuck-Röpke wave function

Qing Zhao,<sup>1,\*</sup> Zhongzhou Ren,<sup>2,†</sup> Mengjiao Lyu,<sup>3,‡</sup> Hisashi Horiuchi,<sup>3,4</sup> Yoshiko Kanada-En'yo,<sup>5,§</sup> Yasuro Funaki,<sup>6</sup> Gerd Röpke,<sup>7</sup> Peter Schuck,<sup>8,9</sup> Akihiro Tohsaki,<sup>3</sup> Chang Xu,<sup>1</sup> Taiichi Yamada,<sup>6</sup> and Bo Zhou<sup>10,11</sup>

<sup>1</sup>*School of Physics and Key Laboratory of Modern Acoustics, Institute of Acoustics, Nanjing University, Nanjing 210093, China*

<sup>2</sup>*School of Physics Science and Engineering, Tongji University, Shanghai 200092, China*

<sup>3</sup>*Research Center for Nuclear Physics (RCNP), Osaka University, Osaka 567-0047, Japan*

<sup>4</sup>*International Institute for Advanced Studies, Kizugawa 619-0225, Japan*

<sup>5</sup>*Department of Physics, Kyoto University, Kyoto 606-8502, Japan*

<sup>6</sup>*Laboratory of Physics, Kanto Gakuin University, Yokohama 236-8501, Japan*

<sup>7</sup>*Institut für Physik, Universität Rostock, D-18051 Rostock, Germany*

<sup>8</sup>*Institut de Physique Nucléaire, Université Paris-Sud, IN2P3-CNRS, UMR 8608, F-91406, Orsay, France*

<sup>9</sup>*Laboratoire de Physique et Modélisation des Milieux Condensés, CNRS-UMR 5493, F-38042 Grenoble Cedex 9, France*

<sup>10</sup>*Institute for International Collaboration, Hokkaido University, Sapporo 060-0815, Japan*

<sup>11</sup>*Department of Physics, Hokkaido University, 060-0810 Sapporo, Japan*



(Received 10 October 2018; revised manuscript received 25 February 2019; published 9 July 2019)

In order to study the nucleon-nucleon pairing effects in clustering nuclei, we formulate a superposed Tohsaki-Horiuchi-Schuck-Röpke (THSR) wave function, which includes both molecular-orbit and pairing configurations explicitly. With this new wave function, we investigate the anomalous deuteronlike  $pn$ -pairing effect in  $^{10}\text{B}$  with  $T = 0$  and  $S = 1$  (isoscalar) by comparing with isovector  $NN$  pairs ( $T = 1, S = 0$ ) in  $^{10}\text{Be}$  and  $^{10}\text{C}$ . Energies are calculated for the ground states of  $^{10}\text{Be}$ ,  $^{10}\text{B}$  and  $^{10}\text{C}$  nuclei, and the  $1^+_10$  excited state of  $^{10}\text{B}$ . These energies are essentially improved comparing with studies using a previous version of THSR wave function. Furthermore, overlaps between the total wave function and the pairing component indicate that the  $NN$  pairing effect is more visible in  $^{10}\text{B}$  than in  $^{10}\text{Be}$  and  $^{10}\text{C}$ . By analyzing the energies and the overlaps between wave function components, we observe two different mechanisms enhancing the formation of deuteronlike pairs in  $^{10}\text{B}$ . We also discuss the pairing effect by showing average distances between components in each nucleus and density distributions of valence nucleons.

DOI: [10.1103/PhysRevC.100.014306](https://doi.org/10.1103/PhysRevC.100.014306)

### I. INTRODUCTION

In atomic nuclei, exotic phenomena are triggered by the formation of  $\alpha$  clusters in the light mass region, and various nuclear theories have been developed for the study of nuclear clustering states [1–8]. The investigation of the nucleon-nucleon ( $NN$ ) pairing effect is one of the most interesting topics in nuclear structure theories [9,10]. Especially, the Bardeen-Cooper-Schrieffer theory (BCS) has revealed that the pairing physics is essential in various nuclear systems, including light nuclei, neutron star matter, as well as in nuclear reactions [11]. Moreover, the coupling of  $\alpha$  clusters and  $NN$  pairs is important for the cluster states of general nuclei composed of both  $\alpha$  clusters and valence nucleons, as discussed in various many-body systems in previous works [12,13]. Hence, the investigation of the  $NN$  pairing effect in cluster states is a meaningful step to improve our present understanding of nuclear clustering effects [14,15].

In recent years, *ab initio* calculations using the no-core shell model (NCSM) approach [16] have been applied to  $A = 10$  nuclei [17], using the effective interactions derived from the two-body ( $NN$ ) and three-body ( $NNN$ ) nuclear forces [18,19]. In these studies, it is concluded that the  $NNN$  force is essential to describe the lower states of  $^{10}\text{B}$ . In studies with effective field theory, the contribution of the  $NNN$  force to the formation of proton-neutron ( $pn$ ) pairs is reproduced if the two-body interaction is reduced [20]. The validity of this estimation is confirmed by AMD calculations of  $^{10}\text{B}$  [9].

There are two kinds of  $NN$  pairs with respect to the isospin symmetry: the isovector pairs with  $T = 1$ , and the isoscalar pairs with  $T = 0$ . The existence of the isospin symmetry requires that the Hamiltonian describing the nuclear system should be invariant under rotations in the isospace [21]. For general nuclei, the isovector pairs are studied intensively, see Ref. [21] and references therein. Deuteronlike isoscalar pairing occurs only rarely because the difference of the neutron and proton Fermi energies must be small compared to the Cooper pair binding energy, and it is less discussed in the literature, see Refs. [6,22–25] and references therein. One important anomaly is the strong isoscalar pairing in the  $^{10}\text{B}$  nucleus where the formation of  $NN$  pairs is strongly

\*zhaqing91@outlook.com

†Corresponding author: zren@tongji.edu.cn

‡mengjiao@rcnp.osaka-u.ac.jp

§yeny@ruby.scphys.kyoto-u.ac.jp

influenced by the coexistent  $\alpha$ -clustering effect [9,10]. Therefore, the mechanism of  $NN$  pairing in  $^{10}\text{B}$  is essential for the understanding of the isoscalar pairing effect in general. Considering the complexity that originate from the coupling of clustering and pairing effects, it is desirable to fix the  $\alpha$ -cluster components in the nuclei and then pin down the modulation of  $NN$  pairing by the spin-isospin channels of two paired nucleons. An ideal approach is to compare the  $NN$  pairing effects in the  $^{10}\text{B}$  nucleus in  $T = 0$  states with  $^{10}\text{Be}$  and  $^{10}\text{C}$  nuclei in  $T = 1$  states. Correspondingly, theoretical descriptions should be formulated for these nuclei to investigate their  $NN$  pairing structures and dynamics of pair motion. The pairing strength obtained from these investigations is also essential for experimental probing of the  $NN$  correlations where the structural information is included as inputs for the prediction of deuteron knockout reaction ( $p$ ,  $pd$ ) observables [26], which are highly sensitive to the peripheral region of the target nucleus [27].

In order to study the different pairs consisting of neutrons ( $nn$ ), protons ( $pp$ ), or proton and neutron ( $pn$ ), we focus on the  $^{10}\text{Be}$ ,  $^{10}\text{B}$  and  $^{10}\text{C}$  nuclei that are all composed of two valence nucleons and two  $\alpha$  clusters. Because of the different configurations of nucleon-pairs among these three nuclei, it is possible to discuss the essential mechanisms for the formation of  $NN$  pairs as well as their different properties, especially for the deuteronlike proton-neutron correlation in  $^{10}\text{B}$ .

To study the pairing effects in these nuclei, we propose a new extended formulation of the Tohsaki-Horiuchi-Schuck-Röpke (THSR) wave function, which is a successful clustering model for various light nuclei [28–31], especially for the Hoyle state ( $0_2^+$ ) in  $^{12}\text{C}$  [28]. By comparing with the generator coordinate method (GCM), the wave function of cluster states are found to be almost 100% accurately described by a single THSR wave function in light nuclei [30–34]. In this work, we propose the extended THSR wave function in superposed form, which we name as THSR + pair wave function. For the first time, an additional pairing configuration for the valence nucleons is introduced into the THSR approach, which provides a convenient framework for the discussion of the  $NN$  pairing effect in nuclear system. With this wave function, we investigate the unfrequent isoscalar  $NN$  pairing effects for the  $^{10}\text{B}$  nucleus and compare with the isovector  $NN$  pairing effects in  $^{10}\text{Be}$  and  $^{10}\text{C}$  nuclei. Moreover, benefiting from the concise intrinsic analytical formulation, the THSR wave function possesses great advantage in discussing the structure and dynamics of  $NN$  pairs in nuclei, as this was done for the  $\alpha$  clusters [31,35] and valence nucleons [13,36,37] in previous works.

This work is organized as follows. In Sec. II, we formulate the THSR + pair wave function for  $^{10}\text{Be}$ ,  $^{10}\text{B}$ , and  $^{10}\text{C}$  nuclei. In Sec. III we provide the numerical results, including the energy, overlaps between components, average distances, density distributions, and corresponding discussions. The final Sec. IV contains the conclusions.

## II. FORMULATION

We consider nuclei with  $A = 10$ , which consist of two  $\alpha$ -like clusters, denoted with index 1, 2, and two additional

nucleons  $a, b$ , which may be neutrons or protons. We start by writing the traditional THSR wave function, which is used in our previous calculations [36],

$$\begin{aligned} \Phi = & \prod_{i=1}^2 \int dR_i \exp\left(-\frac{R_{i,x}^2}{\beta_{\alpha,xy}^2} - \frac{R_{i,y}^2}{\beta_{\alpha,xy}^2} - \frac{R_{i,z}^2}{\beta_{\alpha,z}^2}\right) \\ & \times \int dR_a \exp\left(-\frac{R_{a,x}^2}{\beta_{ab,xy}^2} - \frac{R_{a,y}^2}{\beta_{ab,xy}^2} - \frac{R_{a,z}^2}{\beta_{ab,z}^2}\right) \\ & \times \int dR_b \exp\left(-\frac{R_{b,x}^2}{\beta_{ab,xy}^2} - \frac{R_{b,y}^2}{\beta_{ab,xy}^2} - \frac{R_{b,z}^2}{\beta_{ab,z}^2}\right) \\ & \times e^{im_a\phi_{\mathbf{R}_a}} e^{im_b\phi_{\mathbf{R}_b}} \Phi^{\text{B}}(\mathbf{R}_1, \mathbf{R}_2, \mathbf{R}_a, \mathbf{R}_b), \end{aligned} \quad (1)$$

The terms  $e^{im_a\phi_{\mathbf{R}_a}}$  and  $e^{im_b\phi_{\mathbf{R}_b}}$  are the phase factors, which are introduced to obtain correct parities and orbital angular momenta for the valence nucleons [36]. The Gaussian parameters  $\beta$  constrain the nonlocalized motions of two  $\alpha$  clusters and valence nucleons [36]. We choose the size parameters  $\beta$  for the  $z$  direction and the  $x$ - $y$  direction separately to account for deformation in nuclei. Here, we assume that two valence nucleons share the same value of Gaussian parameters  $\beta$ , which are denoted as  $\beta_{ab}$ . The parameters are determined by variational calculation.  $\Phi^{\text{B}}$  is the Brink wave function defined by [21]

$$\begin{aligned} \Phi^{\text{B}}(\mathbf{R}_1, \mathbf{R}_2, \mathbf{R}_a, \mathbf{R}_b) \\ = \mathcal{A}\{\psi(\alpha_1, \mathbf{R}_1)\psi(\alpha_2, \mathbf{R}_2)\phi(\mathbf{r}_a, \mathbf{R}_a)\phi(\mathbf{r}_b, \mathbf{R}_b)\}, \end{aligned} \quad (2)$$

where the  $\mathbf{R}_{1,2}$  and  $\mathbf{R}_{a,b}$  are corresponding generator coordinates for the  $\alpha$  clusters and valence nucleons, respectively.  $\mathcal{A}$  is the antisymmetrizer and  $\psi(\alpha, \mathbf{R})$  is the wave function of the  $\alpha$  cluster, which is constructed with four single-particle wave functions.

$$\psi(\alpha, \mathbf{R}) = \mathcal{A}\{\phi_1(\mathbf{r}_1, \mathbf{R})\phi_2(\mathbf{r}_2, \mathbf{R})\phi_3(\mathbf{r}_3, \mathbf{R})\phi_4(\mathbf{r}_4, \mathbf{R})\}. \quad (3)$$

The single-particle wave function can be written as

$$\phi(\mathbf{r}, \mathbf{R}) = \left(\frac{2\nu}{\pi}\right)^{3/4} e^{-\nu(\mathbf{r}-\mathbf{R})^2} \chi_\sigma \chi_\tau, \quad (4)$$

where the Gaussian range parameter is given by  $\nu = \frac{1}{2b^2}$ .  $\chi_\sigma$  is the spin part of the nucleon which is up ( $\uparrow$ ) or down ( $\downarrow$ ) in the  $z$  direction.  $\chi_\tau$  is the isospin part of the proton ( $p$ ) or the neutron ( $n$ ).

The above traditional THSR wave function in Eq. (1) provides a good description for the molecular-orbit configurations but does not include directly the  $NN$  pairing structure. In pioneering works, many studies indicate that the two valence nucleons have a trend to form  $NN$  pairs in  $^{10}\text{Be}$ ,  $^{10}\text{B}$ , and  $^{10}\text{C}$  nuclei [9,12]. In order to describe this component and provide a clear description for the pair structure, we introduce an additional compact  $NN$  pairing term as

$$\begin{aligned} \Phi_p = & \prod_{i=1}^2 \int dR_i \exp\left(-\frac{R_{i,x}^2}{\beta_{\alpha,xy}^2} - \frac{R_{i,y}^2}{\beta_{\alpha,xy}^2} - \frac{R_{i,z}^2}{\beta_{\alpha,z}^2}\right) \\ & \times \int dR_{\text{pair}} \exp\left(-\frac{R_{\text{pair},x}^2}{\beta_{\text{pair},xy}^2} - \frac{R_{\text{pair},y}^2}{\beta_{\text{pair},xy}^2} - \frac{R_{\text{pair},z}^2}{\beta_{\text{pair},z}^2}\right) \\ & \times e^{im_a\phi_{\mathbf{R}_{\text{pair}}}} e^{im_b\phi_{\mathbf{R}_{\text{pair}}}} \Phi^{\text{B}}(\mathbf{R}_1, \mathbf{R}_2, \mathbf{R}_{\text{pair}}). \end{aligned} \quad (5)$$

In this term, we treat valence nucleons as a two-particle cluster, which share the same generate coordinate  $\mathbf{R}_{\text{pair}}$ , so that the corresponding Brink wave function can be written as

$$\begin{aligned} \Phi^{\text{B}}(\mathbf{R}_1, \mathbf{R}_2, \mathbf{R}_{\text{pair}}) \\ = \mathcal{A}\{\psi(\alpha_1, \mathbf{R}_1)\psi(\alpha_2, \mathbf{R}_2)\psi(\alpha_{\text{pair}}, \mathbf{R}_{\text{pair}})\}, \end{aligned} \quad (6)$$

where  $\psi(\alpha_{\text{pair}}, \mathbf{R}_{\text{pair}})$  is the wave function of the  $NN$  pair, which contains two single-particle wave functions (product of two Gaussians), see Eq. (3). This corresponds to a compact pairing configuration in  $^{10}\text{Be}$ ,  $^{10}\text{B}$ , and  $^{10}\text{C}$ . The relative motion inside the pair can be described by combining the unpaired molecular-orbit configuration with this compact pairing configuration. So, we formulate the THSR + pair wave function as a superposition of the molecular-orbit configuration  $\Phi$  in Eq. (1) and this additional term  $\Phi_p$ , as

$$\Psi_{\text{pair}} = c\Phi + d\Phi_p. \quad (7)$$

Here  $c$  and  $d$  are the coefficients, which are determined by variational calculations. There is only one degree of freedom, which is the ratio  $c/d$ , as the actual variational parameter because of normalization. The parameters  $m_a$  and  $m_b$  in the phase factors  $e^{im_a\phi_{\mathbf{R}_a}}$  and  $e^{im_b\phi_{\mathbf{R}_b}}$  are chosen according to the rotational symmetry of the nuclear state under consideration [13,36]. For the  $0^+$  ground state of  $^{10}\text{Be}$  and  $^{10}\text{C}$ , we choose  $m_a = 1$  and  $m_b = -1$  in Eqs. (1) and (5) to describe the antiparallel couplings of spins for the two valence nucleons around two  $\alpha$  clusters. We note that under this condition the phase factors in Eq. (5) vanish and the pair wave function  $\Phi_p$  is reduced to the  $S$  wave. As for the  $3^+$  ground state of  $^{10}\text{B}$ , the parameters are chosen as  $m_a = m_b = 1$ , which describes the parallel couplings of spins between valence nucleons.

We apply the angular-momentum projection technique  $\hat{P}_{MK}^J|\Psi\rangle$  to restore the rotational symmetry [38],

$$\begin{aligned} |\Psi^{JM}\rangle &= \hat{P}_{MK}^J|\Psi\rangle \\ &= \frac{2J+1}{8\pi^2} \int d\Omega D_{MK}^{J*}(\Omega) \hat{R}(\Omega)|\Psi\rangle, \end{aligned} \quad (8)$$

where  $J$  is the total angular momentum of the system. For the  $3_1^+0$  ground state and  $1_1^+0$  excited state of  $^{10}\text{B}$  with isospin  $T=0$ , we take the isospin projection by using the proton-neutron exchange operator  $\hat{P}_{p\leftrightarrow n}$  as introduced in Refs. [9,10].

The Hamiltonian of the  $A=10$  nuclear systems can be written as

$$H = \sum_{i=1}^{10} T_i - T_{c.m.} + \sum_{i<j}^{10} V_{ij}^N + \sum_{i<j}^{10} V_{ij}^C + \sum_{i<j}^{10} V_{ij}^{ls}. \quad (9)$$

We use the Volkov No. 2 interaction given in Ref. [39] for the central force, which is selected as

$$V_{ij}^N = \{V_1 e^{-\alpha_1 r_{ij}^2} - V_2 e^{-\alpha_2 r_{ij}^2}\} \{W - M\hat{P}_\sigma \hat{P}_\tau + B\hat{P}_\sigma - H\hat{P}_\tau\}, \quad (10)$$

where  $M = 0.6$ ,  $W = 0.4$ ,  $B = H = 0.125$ ,  $V_1 = -60.650$  MeV,  $V_2 = 61.140$  MeV,  $\alpha_1 = 0.309$  fm $^{-2}$ , and  $\alpha_2 = 0.980$  fm $^{-2}$ . The G3RS (Gaussian soft core potential with three ranges) term [40], which is a two-body type interaction,

TABLE I. Energies of the ground states for  $^{10}\text{Be}$ ,  $^{10}\text{B}$ , and  $^{10}\text{C}$ .  $E^{\text{THSR}}$  denotes energies obtained from the THSR wave function,  $E^{\text{THSR+pair}}$  denotes results obtained from the THSR+pair wave function.  $\Delta$  indicates the improvement of energies in the new THSR+pair wave function compared to the values obtained from previous version of THSR wave function. All units of energies are in MeV.

	$^{10}\text{Be}(0^+1)$	$^{10}\text{B}(3^+0)$	$^{10}\text{C}(0^+1)$
$E^{\text{exp}}$ [45]	-65.0	-64.8	-60.3
$E^{\text{THSR}}$	-58.3	-59.8	-54.4
$E^{\text{THSR+pair}}$	-59.2	-61.8	-55.3
$\Delta$	0.9	2.0	0.9

is taken as the spin-orbit interaction as

$$V_{ij}^{ls} = V_0^{ls} \{e^{-\alpha_1 r_{ij}^2} - e^{-\alpha_2 r_{ij}^2}\} \mathbf{L} \cdot \mathbf{S} \hat{P}_{31}, \quad (11)$$

where  $\hat{P}_{31}$  projects the two-body system into triplet odd state and the parameters are set to be  $V_0^{ls} = 1600$  MeV,  $\alpha_1 = 5.00$  fm $^{-2}$  and  $\alpha_2 = 2.778$  fm $^{-2}$ . The Gaussian width parameter  $b$  of single-particle wave functions is chosen as  $b = 1.46$  fm, which reproduces nicely the spectrum of  $^9\text{Be}$  and  $^{10}\text{Be}$  nuclei in the MO, AMD, and dineutron condensation model calculations [41–44].

### III. RESULTS AND DISCUSSION

We calculate the ground-state energies of  $^{10}\text{Be}$ ,  $^{10}\text{B}$ , and  $^{10}\text{C}$  by variational optimization of parameters in the THSR + pair wave function. The corresponding energy results are shown in Table I, where corresponding experimental data [45] and results calculated with the traditional THSR wave function  $\Phi$  in Eq. (1) are also included. The masses of proton and neutron in the single-particle wave function are set to be equal to experimental values in Ref. [46].

From the comparison in Table I, it is clearly observed that the ground-state energies of  $^{10}\text{Be}$ ,  $^{10}\text{B}$ , and  $^{10}\text{C}$  are greatly improved by additional superposition of the pair term  $\Phi_p$  in Eq. (2) in the THSR + pair wave function  $\Psi_{\text{pair}}$ . For  $^{10}\text{B}$ , the THSR + pair wave function improves the ground-state energy by about 2.0 MeV compared to the traditional THSR wave function, which is more significant than the improvements for other two nuclei. These results show that the  $NN$  pairing structure is essential for the precise description of the  $^{10}\text{B}$  nucleus. To explain the effect of the pairing component, we give further discussions in Appendix Sec. A 2.

In order to investigate the  $NN$  pairing configuration in the THSR + pair wave function, we calculate the overlap between molecular-orbit term  $\Phi$  and the total THSR + pair wave function  $\Psi_{\text{pair}}$ , the overlap between pairing term  $\Phi_p$  and the total THSR + pair wave function  $\Psi_{\text{pair}}$ , as well as the overlap between molecular-orbit term  $\Phi$  and pairing term  $\Phi_p$ . Corresponding results are shown in Table II. From this table, we observe that the overlaps between the molecular-orbit term and THSR + pair wave function are larger than 90% for all of  $^{10}\text{Be}$ ,  $^{10}\text{B}$ , and  $^{10}\text{C}$  nuclei. These large overlaps indicate that the molecular-orbit term could provide a good description for these nuclei. However, additional pairing term

TABLE II. The overlaps between each two of the THSR+pair wave function  $\Psi_{\text{pair}}$  and its two components  $\Phi$  and  $\Phi_p$  of molecular-orbit configuration and pairing configuration, respectively. Values are calculated for the ground states of  $^{10}\text{Be}$ ,  $^{10}\text{B}$ , and  $^{10}\text{C}$  nuclei. All the wave functions  $\Phi$ ,  $\Phi_p$ , and  $\Psi_{\text{pair}}$  have been normalized.

	$^{10}\text{Be}(0^+1)$	$^{10}\text{B}(3^+0)$	$^{10}\text{C}(0^+1)$
$\langle \Phi   \Psi_{\text{pair}} \rangle^2$	92.9%	90.8%	93.6%
$\langle \Phi_p   \Psi_{\text{pair}} \rangle^2$	56.6%	93.3%	67.5%
$\langle \Phi   \Phi_p \rangle^2$	45.5%	75.8%	43.1%

is still necessary to obtain accurate wave function as these overlaps do not equal 100%. It is also observed that the overlaps  $\langle \Phi_p | \Psi_{\text{pair}} \rangle^2$  are different among  $^{10}\text{Be}$ ,  $^{10}\text{B}$ , and  $^{10}\text{C}$ , where the overlap for  $^{10}\text{B}$  nucleus is significantly larger than for the other two nuclei. Hence the optimized THSR + pair wave describes stronger  $NN$  pairing effect in  $^{10}\text{B}$  than those in  $^{10}\text{Be}$  and  $^{10}\text{C}$  as we concluded previously. From the large ratio  $\langle \Phi | \Phi_p \rangle^2 = 75.8\%$ , we found that molecular-orbit term  $\Phi$  in the  $3^+0$  ground state of  $^{10}\text{B}$  provides the description that is analogous to the pairing term  $\Phi_p$ , which explains the strong pairing effect in this state.

In order to eliminate the effect of orbital angular momentum, we also calculate the  $1_1^+0$  excited state of  $^{10}\text{B}$ , which is the spin-isospin partner for the  $0_1^+$  ground states of  $^{10}\text{Be}$  and  $^{10}\text{C}$  nuclei, as they all have dominant  $L = 0$  components that originate from the antiparallel coupling of orbital angular momentum of two valence nucleons [9,10]. Hence, the total spin  $S$  and isospin  $T$  of two valence nucleons are the only differences among the  $1_1^+0$  excited state of  $^{10}\text{B}$  and the  $0_1^+$  ground states of  $^{10}\text{Be}$  and  $^{10}\text{C}$ . In Table III, we show the energies of the  $1_1^+$  excited state calculated with the traditional THSR wave function  $\Phi$  and the THSR + pair wave function  $\Psi_{\text{pair}}$ . In these calculations, we set parameters  $m_{ab} = \pm 1$ , respectively, for two valence nucleons to describe the antiparallel coupling of orbital angular momenta. The corresponding experimental data adopted from Ref. [45] are also included for comparison. From this table, it is observed that the excitation energy of the  $1_1^+0$  state is improved from 2.8–1.0 MeV by adding the pairing term, which is much closer to the experimental value 0.7 MeV. It is also clearly shown that the introduction of the

TABLE III. Energies of the  $3^+0$  ground state and the  $1_1^+0$  excited state for  $^{10}\text{B}$ .  $E^{\text{THSR}}$  denotes energies obtained from the THSR wave function.  $E^{\text{THSR+pair}}$  denotes results obtained from the THSR+pair wave function.  $\Delta$  denotes the improvement of energies in the new THSR+pair wave function compared to the values obtained from traditional THSR wave function.  $E^{\text{exp}}$  denotes experimental values adopted from Ref. [45].  $E_{\text{ex}}$  denotes the corresponding excited energies. All units of energies are in MeV.

$^{10}\text{B}$	$3^+0$	$1_1^+0$	$E_{\text{ex}}$
$E^{\text{exp}}$	−64.8	−64.1	0.7
$E^{\text{THSR}}$	−59.8	−57.0	2.8
$E^{\text{THSR+pair}}$	−61.8	−60.8	1.0
$\Delta$	2.0	3.8	1.8

TABLE IV. The overlaps between each two of the THSR+pair wave function  $\Psi_{\text{pair}}$  and its two components  $\Phi$  and  $\Phi_p$  of molecular-orbit configuration and pairing configuration, respectively. Values are calculated for the ground states of  $^{10}\text{Be}$  and  $^{10}\text{C}$  nuclei and the  $1_1^+0$  excited state of  $^{10}\text{B}$ . All the wave functions  $\Phi$ ,  $\Phi_p$ , and  $\Psi_{\text{pair}}$  are normalized.

	$^{10}\text{Be}(0^+1)$	$^{10}\text{C}(0^+1)$	$^{10}\text{B}(1_1^+0)$
$\langle \Phi   \Psi_{\text{pair}} \rangle^2$	92.9%	93.6%	83.7%
$\langle \Phi_p   \Psi_{\text{pair}} \rangle^2$	56.6%	67.5%	87.5%
$\langle \Phi   \Phi_p \rangle^2$	45.5%	43.1%	55.8%

additional pairing term  $\Phi_p$  improves the energy of the  $1_1^+0$  excited state by about 3.8 MeV, which is significantly larger than the corresponding improvement of about 2.0 MeV for the  $3^+0$  ground state.

This improvement of 3.8 MeV is also significantly larger than corresponding values for the  $0_1^+1$  ground states of  $^{10}\text{Be}$  and  $^{10}\text{C}$ , as shown in Table I. Hence we observe the enhanced pairing effect again in the  $1_1^+0$  state of  $^{10}\text{B}$  with  $T = 0$  compared to the pairs with  $T = 1$  in  $^{10}\text{Be}$  and  $^{10}\text{C}$ . However, the previous explanation for the pairing effect in the  $3^+0$  ground state of  $^{10}\text{B}$  no longer persists, because the analogy between the molecular-orbit configuration and pairing configuration is much weaker in the  $1_1^+0$  state. This is demonstrated in Table IV where the overlap between the molecular-orbit term  $\Phi$  and the pairing term  $\Phi_p$  in this state is found to be 55.8%, which is much smaller than the corresponding value of 75.8% in the  $3^+0$  ground state. From this we conclude that these two configurations compete with each other in the  $1_1^+0$  state, which is different from the analogous contribution in the total wave function.

As listed in Table IV, the squared overlaps between the molecular-orbit term  $\Phi$  and total wave function  $\Psi_{\text{pair}}$  in the  $T = 1$  states of  $^{10}\text{Be}$  and  $^{10}\text{C}$  are larger than 90%, which shows that the molecular-orbit configuration prevails in these states. This can be explained by the fact that the molecular-orbit configuration is energetically favorable in the  $T = 1$  nuclei  $^{10}\text{Be}$  and  $^{10}\text{C}$ , where both of the molecular orbits have parallel spin-orbit coupling and provide large contributions to the total energies of nuclei. In contrary, the spin-orbit contributions from valence nucleons is canceled among each other in the pairing configuration, as the two paired nucleons have opposite spin directions but the same orbital motion. In the  $1_1^+0$  excited state of  $^{10}\text{B}$  the dominance of molecular-orbit configuration disappears, as shown by the larger overlap 87.5% between pairing configuration  $\Phi_p$  and total wave function  $\Psi_{\text{pair}}$ . In the molecular-orbit term  $\Phi$  of this state, the spin-orbit coupling is parallel and antiparallel for the two valence nucleons, respectively. Hence there is also cancellation of spin-orbit contribution from valence nucleons, which is similar to the case in the pairing configuration. As a consequence, the molecular-orbit configuration is not energetically favorable and it is quenched in the total wave function by its competition with the pairing configuration in the  $1_1^+0$  excited state of  $^{10}\text{B}$ .

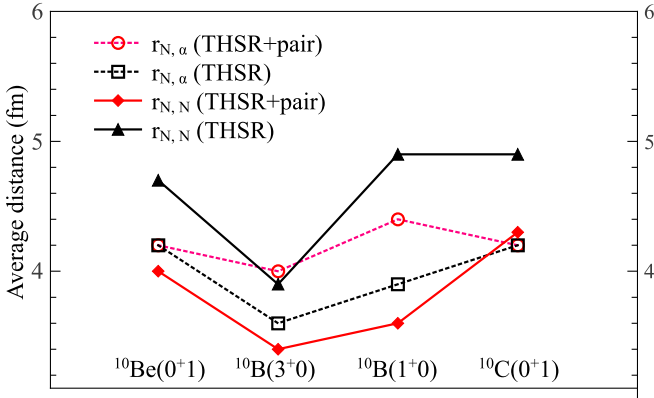


FIG. 1. The average distances between nucleons in  $^{10}\text{Be}(0^+1)$ ,  $^{10}\text{B}(3^+0)$ ,  $^{10}\text{B}(1^+0)$ , and  $^{10}\text{C}(0^+1)$  states. The solid lines denote the average distances  $r_{N,N}$  between two valence nucleons. The dashed lines denote the average distances  $r_{N,\alpha}$  between valence nucleons and the center of two  $\alpha$  clusters. For both the solid lines and dashed lines, the black color denotes results obtained by using only the molecular-orbit configuration  $\Phi$  and the red color denotes results from the total THSR + pair wave function  $\Psi_{\text{pair}}$ . All units are in fm.

The  $NN$  pairing is formulated in the deuteronlike channels ( $T = 0, S = 1$ ) of two valence nucleons both for the  $3^+0$  ground state and for the  $1^+0$  excited state of  $^{10}\text{B}$ . However, the  $NN$  pairs are distinct by two different mechanisms in these states: For the  $3^+0$  ground state, the molecular-orbit configuration of two valence nucleons is analogous to the pairing configuration and hence enhances the possibility of  $NN$  pairing. In the  $1^+0$  excited state of  $^{10}\text{B}$ , molecular-orbit configuration competes with the pairing configuration and hence it is quenched compared with its dominance in the  $0^+1$  states of  $^{10}\text{Be}$  and  $^{10}\text{C}$ . On the other hand the latter encourages the formation of  $NN$  pairing.

The  $NN$  pair structure in  $^{10}\text{Be}$ ,  $^{10}\text{B}$ , and  $^{10}\text{C}$  can be demonstrated explicitly by showing the average distances between the two valence nucleons, which correspond to the average sizes of  $NN$  pairs. It should be noticed that the formation of  $NN$  pairs can affect both the distance between two valence nucleons  $r_{N,N}$  and the distance between  $NN$  pair and the center of two  $\alpha$  clusters  $r_{N,\alpha}$ . Hence when the strength of  $NN$  pairing effect increases, the ratio  $r_{N,N}/r_{N,\alpha}$  is reduced to a relatively small value. We compare the average distances for  $^{10}\text{Be}$ ,  $^{10}\text{B}$ , and  $^{10}\text{C}$  in Fig. 1, including the  $1^+0$  state of  $^{10}\text{B}$ . As shown in this figure, with the molecular-orbit configurations (the black lines), the  $NN$  distances  $r_{N,N}$  have almost the same magnitude as  $r_{N,\alpha}$  for all nuclei of  $^{10}\text{Be}$ ,  $^{10}\text{B}$ , and  $^{10}\text{C}$ , which is due to the absence of the pairing term in the molecular-orbit configuration. With the new extended THSR + pair wave function (the red lines), the  $r_{N,N}$  in  $^{10}\text{Be}$  is smaller but comparable to  $r_{N,\alpha}$ , showing a relatively weak  $NN$  pairing effect in  $^{10}\text{Be}$ . For  $^{10}\text{C}$ , the  $NN$  pairing effect is even weaker as the corresponding  $r_{N,N}$  is larger than  $r_{N,\alpha}$ . We see a significantly small ratio  $r_{N,N}/r_{N,\alpha}$  for both states of  $^{10}\text{B}$  nucleus where the  $NN$  pairing effect is stronger, as discussed previously. We also see that the ratio  $r_{N,N}/r_{N,\alpha}$  for the  $1^+0$  excited state of  $^{10}\text{B}$  is smaller than the one for the  $3^+0$  ground

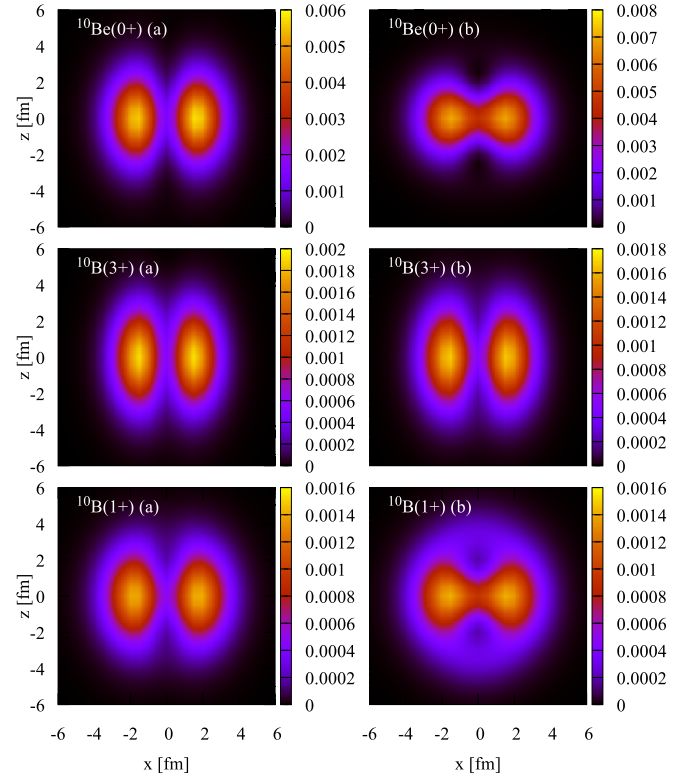


FIG. 2. The density distributions of the valence nucleons in the  $x - z$  plane for the  $0^+1$  state of  $^{10}\text{Be}$ , the  $3^+0$  state of  $^{10}\text{B}$  and the  $1^+0$  state of  $^{10}\text{B}$ . The panels (a) are calculated with the THSR + pair wave function  $\Psi_{\text{pair}}$  with optimized parameters. The panels (b) are obtained by using only the pairing term  $\Phi_p$  with parameter  $c = 0$ . For all these calculations,  $\beta$  parameters are set to optimized values in the corresponding THSR + pair wave functions.

state, which indicates a relative weaker pairing effect for the  $1^+0$  state.

In order to investigate the nuclear dynamics of  $NN$  pairs, we calculate the density distributions for valence nucleons of the  $0^+1$  ground state of  $^{10}\text{Be}$ , the  $3^+0$  ground state of  $^{10}\text{B}$  and  $1^+0$  excited state of  $^{10}\text{B}$ , as shown in Fig. 2. In this figure, panels labeled by (a) are calculated with the THSR + pair wave function  $\Psi_{\text{pair}}$ . The panels labeled by (b) are calculated by using only the pairing term  $\Phi_p$ . For all these wave functions,  $\beta$  parameters are set to optimized values in corresponding THSR + pair wave functions.

From Fig. 2, we observe that the valence nucleons in the  $3^+0$  ground state of  $^{10}\text{B}$  have narrow distributions in the  $x$ - $y$  direction because it is tightly bounded by the spin-orbit potential and the centrifugal barrier. While in the cases of the ground state of  $^{10}\text{Be}$  and the  $1^+0$  excited state of  $^{10}\text{B}$ , the distributions of the valence nucleons are broader because of the weaker spin-orbit potential and lower centrifugal barrier. This result agrees with the conclusions in Ref. [10] and Ref. [47]. By comparing the panels (b) in these figures, we notice that when no centrifugal barrier exists, as in the  $0^+1$  state of  $^{10}\text{Be}$  and  $1^+0$  state of  $^{10}\text{B}$ , the  $NN$  pairs described by the pairing term  $\Phi_p$  have a wider distribution near the  $z = 0$  cross section between two  $\alpha$  clusters, which corresponds to

TABLE V. The variationally optimized  $\beta$  parameters for the wave function of  $^{10}\text{Be}$  ( $0^+1$ ),  $^{10}\text{B}$  ( $3^+0$ ),  $^{10}\text{B}$  ( $1^+0$ ), and  $^{10}\text{C}$  ( $0^+1$ ). For each nucleus, the top line corresponds to the calculation with traditional THSR wave function  $\Phi$  and the bottom line denoted by symbol “ $\hookrightarrow$ ” corresponds to calculation with THSR+pair wave function  $\Psi_{\text{pair}}$ . The units of  $\beta$  parameters are in fm.

Nucleus	$\beta_{\alpha,xy}$	$\beta_{\alpha,z}$	$\beta_{ab,xy}$	$\beta_{ab,z}$	$\beta_{\text{pair},xy}$	$\beta_{\text{pair},z}$	$c/d$
$^{10}\text{Be}$ ( $0^+1$ )	0.1	2.5	1.9	2.9	/	/	/
$\hookrightarrow$	0.1	2.8	1.9	3.3	2.5	0.8	8.09
$^{10}\text{B}$ ( $3^+0$ )	0.1	1.9	1.1	2.2	/	/	/
$\hookrightarrow$	0.1	2.6	1.0	3.2	1.8	3.3	3.35
$^{10}\text{B}$ ( $1^+0$ )	0.1	2.2	2.2	2.0	/	/	/
$\hookrightarrow$	0.1	3.0	2.4	2.8	3.0	2.7	3.35
$^{10}\text{C}$ ( $0^+1$ )	0.1	2.8	2.2	3.3	/	/	/
$\hookrightarrow$	0.1	3.0	2.4	3.2	2.5	0.2	8.09

a relatively dilute three-clusters structure of  $\alpha + \alpha + \text{pair}$ . On the other hand, in the  $3^+0$  ground state of  $^{10}\text{B}$ , the strong spin-orbit coupling to orbital angular momentum  $L = 2$  encourages the spreading of valence nucleons in the  $z$  direction around the  $\alpha$  clusters to formulate  $\pi$ -molecular orbits, as also discussed in Refs. [13,36].

Here we list the optimum parameters of the THSR + pair wave function and the traditional THSR wave function in Table V for each state. The parameters  $\beta$  denote the motions of  $\alpha$  clusters and the valence nucleons, which can be reflected in density distributions. Therefore, we can make similar conclusions from this table.

#### IV. CONCLUSION

A new extended formulation of THSR wave function, named as THSR + pair wave function, for  $^{10}\text{Be}$ ,  $^{10}\text{B}$ , and  $^{10}\text{C}$  nuclei has been proposed in this work. In this wave function, an  $NN$  pairing term is introduced in addition to the molecular-orbit term used in the previous version of THSR wave function. By using the THSR + pair wave function, the energies for the ground states are improved significantly for these nuclei, especially for the  $^{10}\text{B}$  nucleus. Analyses of energies and overlaps show that the pair configuration is stronger in the  $^{10}\text{B}$  nucleus compared to the other two nuclei. We also calculate the  $1^+0$  excited state of  $^{10}\text{B}$  using the THSR + pair wave functions and observe again a strong pairing effect in this state. These results show that pairing effects are enhanced in the deuteronlike channel  $S = 1, T = 0$ . From the energies and overlaps between wave function components, we found

TABLE VI. The spin-orbit coupling of valence nucleons in the intrinsic wave functions of  $^{10}\text{Be}$ ,  $^{10}\text{B}$ , and  $^{10}\text{C}$ .  $l_z$  is the orbital angular momentum in  $z$  direction, which is determined by the parameter “ $m$ ” in the phase factor  $e^{im\phi}$  as explained in Eq. (1). Arrows denote the spin components of valence nucleons in  $z$  directions.

	Coupling
$^{10}\text{Be}(0^+1)$	$ l_{z,1} = +1s_{z,1} = \uparrow, l_{z,2} = -1s_{z,1} = \downarrow\rangle \oplus  l_{z,1} = +1s_{z,1} = \downarrow, l_{z,2} = -1s_{z,1} = \uparrow\rangle$
$^{10}\text{C}(0^+1)$	$ l_{z,1} = +1s_{z,1} = \uparrow, l_{z,2} = -1s_{z,1} = \downarrow\rangle \oplus  l_{z,1} = +1s_{z,1} = \downarrow, l_{z,2} = -1s_{z,1} = \uparrow\rangle$
$^{10}\text{B}(3^+0)$	$ l_{z,1} = +1s_{z,1} = \uparrow, l_{z,2} = +1s_{z,1} = \uparrow\rangle$
$^{10}\text{B}(1^+0)$	$ l_{z,1} = +1s_{z,1} = \uparrow, l_{z,2} = -1s_{z,1} = \uparrow\rangle$

that there are two different mechanisms that enhance the formation of  $NN$  pair in  $^{10}\text{B}$  nucleus. In the  $3^+0$  ground state, the strong pairing effect originates from the analogy between molecular-orbit configuration and pairing configuration. In the  $1^+0$  excited state, the pairing configuration competes with molecular-orbit configuration and the molecular-orbit term is energetically unfavored and quenched. We also discuss the structure of  $NN$  pairs and their dynamics of motion in space, by calculating the average distances between their components and the density distributions of valence nucleons. This study further improves the understanding of the formation of  $NN$  pairs and their properties, especially for those in isoscalar channels, which could be beneficial for future investigations of  $NN$  correlations and general cluster states composed of both  $\alpha$  clusters and  $NN$  pairs.

#### ACKNOWLEDGMENTS

The authors would like to thank Dr. Wan for fruitful discussions. This work is supported by the National Natural Science Foundation of China (Grants No. 11535004, No. 11375086, No. 11120101005, No. 11822503, No. 11575082, No. 11761161001), by the National Major State Basic Research and Development of China, Grant No. 2016YFE0129300, by the Science and Technology Development Fund of Macao under Grant No. 068/2011/A, and by the JSPS KAKENHI Grant No. JP16K05351.

#### APPENDIX: DETAILS ABOUT THE SPIN-ORBIT COUPLING AND VARIATIONAL CALCULATIONS

We explain more details of the spin-orbit coupling of the states of  $^{10}\text{Be}$ ,  $^{10}\text{B}$ , and  $^{10}\text{C}$  nuclei. We also discuss the results and minima in the variational calculations.

##### 1. Spin-orbit coupling

In Table. VI, we explain the details of spin-orbit coupling before the angular momentum projection in the intrinsic wave functions. For  $^{10}\text{Be}(0^+1)$  state and  $^{10}\text{C}(0^+1)$  state, we superpose the  $|l_{z,1} = +1, s_{z,1} = \uparrow; l_{z,2} = -1, s_{z,1} = \downarrow\rangle$  configuration of two valence nucleons with the  $|l_{z,1} = +1, s_{z,1} = \downarrow; l_{z,2} = -1, s_{z,1} = \uparrow\rangle$  configuration to describe the  $NN$  pair moving in the  $L = 0$  wave. The coefficients of these two configurations are treated as variational coefficients, which are optimized to be 0.9 and 0.1, respectively. This means that the  $|l_{z,1} = +1s_{z,1} = \uparrow, l_{z,2} = -1s_{z,1} = \downarrow\rangle$  configuration is dominant in  $^{10}\text{Be}(0^+1)$

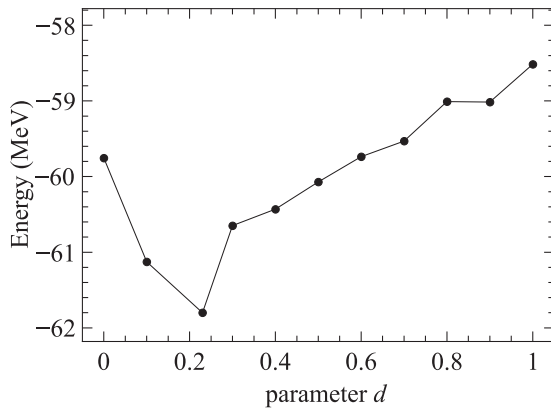


FIG. 3. Energy curve of the  $^{10}\text{B}(3^+0)$  with respect to the parameter  $d$ . The parameter  $c$  is set to be  $d = 1 - c$ . Other parameters are fixed at the optimized values.

and  $^{10}\text{C}(0^+1)$ . For  $^{10}\text{B}(3^+0)$  state and  $^{10}\text{B}(1_1^+0)$  state, we assume  $|l_{z,1} = +1s_{z,1} = \uparrow, l_{z,2} = +1s_{z,1} = \uparrow\rangle$  configuration and  $|l_{z,1} = +1s_{z,1} = \uparrow, l_{z,2} = -1s_{z,1} = \uparrow\rangle$  configuration, respectively. For the  $(1^+0)$  excited state of  $^{10}\text{B}$ , we assume that the  $|l_{z,1} = +1s_{z,1} = \uparrow, l_{z,2} = -1s_{z,1} = \uparrow\rangle$  configuration is dominant and other configurations are neglected.

## 2. Discussion of energy improvements

The improvements of energies can come from the increasing number of parameters, but also due to the additional pairing structure in wave function. As a study of comparison, we superpose two molecular-orbit terms  $\Phi$  and  $\Phi'$  in notation of Eq. (7) as

$$\Psi_{\text{example}} = c\Phi + d\Phi'. \quad (\text{A1})$$

The corresponding  $\beta$  parameters within  $\Phi$  and  $\Phi'$  converge to identical values, and the superposed wave function  $\Psi_{\text{example}}$  reduces to the traditional THSR wave function. This situation will not happen in THSR + pair wave function. We make the variational calculation for the Gaussian parameters  $\beta$  in  $\Phi$  and  $\Phi_p$ , which determine the distribution of the valence nucleons and clusters. However, in order to describe the pairing structure, we let the generator coordinates of the valence nucleons in  $\Phi_p$  have the condition that  $\mathbf{R}_a = \mathbf{R}_b = \mathbf{R}_{\text{pair}}$ . Therefore, the molecular-orbit term  $\Phi$  can not reduce to the pairing term  $\Phi_p$  through the variation of parameters  $\beta$ . The difference between these two terms ensures the effectiveness of the additional pairing structure, and the energy improvement is mostly due to the pairing effect.

## 3. Minimum in variational calculations

We further discuss the variational properties for the parameters used in present framework. We make the full variational calculation for all the parameters simultaneously including the ratio  $c/d$ . For the parameters  $\beta$ , the properties of energy surfaces in the parameter space have been discussed in detail in previous work in Ref. [36], where the minimum is confirmed by the contour maps, which shows that there is only one minimum with parameters  $\beta$ . We further check the energy minimum for the parameter  $c/d$  in the variational calculation of  $^{10}\text{B}(3^+0)$ , as shown in Fig. 3. In this calculation, we set the parameter  $d = 1 - c$  (a mathematical technique to make the variational calculation) and vary the ratio  $c/d$  with respect to parameter  $d$  from 0–1. Parameters  $\beta$  are all fixed as the corresponding optimized values. In this figure, we observe a unique minimum at  $c/d \approx 0.23$ . The variational calculations results and the corresponding discussions on the property of the parameters indicate that the local minimum found in Fig. 3 could be the global minimum.

- 
- [1] M. Freer, H. Horiuchi, Y. Kanada-En'yo, D. Lee, and Ulf-G. Meißner, *Rev. Mod. Phys.* **90**, 035004 (2018).
  - [2] N. Itagaki, S. Okabe, and K. Ikeda, *Prog. Theor. Phys. Suppl.* **142**, 297 (2001).
  - [3] W. von Oertzen, M. Freer, and Y. Kanada-En'yo, *Phys. Rep.* **432**, 43 (2006).
  - [4] Y. Kanada-En'yo, M. Kimura, and A. Ono, *Prog. Theor. Exp. Phys.* **2012**, 01A202 (2012).
  - [5] H. Horiuchi, K. Ikeda, and K. Katō, *Prog. Theor. Phys. Suppl.* **192**, 1 (2012).
  - [6] M. Ito and K. Ikeda, *Rep. Prog. Phys.* **77**, 096301 (2014).
  - [7] P. Navrátil, S. Quaglioni, G. Hupin, C. Romero-Redondo, and A. Calci, *Phys. Scr.* **91**, 053002 (2016).
  - [8] Z. Ren and B. Zhou, *Front. Phys.* **13**, 132110 (2018).
  - [9] Y. Kanada-En'yo and H. Morita, F. Kobayashi, *Phys. Rev. C* **91**, 054323 (2015).
  - [10] H. Morita and Y. Kanada-En'yo, *Prog. Theor. Exp. Phys.* **103D02** (2016).
  - [11] R. A. Broglia and V. Zelevinsky, *Fifty Years of Nuclear BCS: Pairing in Finite Systems* (World Scientific Publishing, Singapore, 2013).
  - [12] F. Kobayashi and Y. Kanada-En'yo, *Phys. Rev. C* **89**, 024315 (2014).
  - [13] M. Lyu, Z. Ren, B. Zhou, Y. Funaki, H. Horiuchi, G. Röpke, P. Schuck, A. Tohsaki, C. Xu, and T. Yamada, *Phys. Rev. C* **93**, 054308 (2016).
  - [14] C. Xu and Z. Ren, *Phys. Rev. C* **73**, 041301(R) (2006).
  - [15] Yuejiao Ren and Zhongzhou Ren, *Phys. Rev. C* **85**, 044608 (2012).
  - [16] R. Machleidt and D. R. Entem, *Phys. Rep.* **503**, 1 (2011).
  - [17] P. Navrátil, V. G. Gueorguiev, J. P. Vary, W. E. Ormand, and A. Nogga, *Phys. Rev. Lett.* **99**, 042501 (2007).
  - [18] E. Epelbaum, A. Nogga, W. Glöckle, H. Kamada, Ulf-G. Meißner, and H. Witala, *Phys. Rev. C* **66**, 064001 (2002).
  - [19] D. R. Entem and R. Machleidt, *Phys. Rev. C* **68**, 041001(R) (2003).
  - [20] M. Kohno, *Phys. Rev. C* **86**, 061301(R) (2012).
  - [21] D. M. Brink and R. A. Broglia, *Nuclear Superfluidity: Pairing in Finite Systems* (Cambridge University Press, New York, 2005), p. 69.

- [22] S. Frauendorf and A. O. Macchiavelli, *Prog. Part. Nucl. Phys.* **78**, 24 (2014).
- [23] G. Röpke, A. Schnell, P. Schuck, and U. Lombardo, *Phys. Rev. C* **61**, 024306 (2000).
- [24] W. Guo, U. Lombardo, and P. Schuck, *Phys. Rev. C* **99**, 014310 (2019).
- [25] A. L. Goodman, *Phys. Rev. C* **63**, 044325 (2001).
- [26] Y. Chazono (private communication).
- [27] K. Yoshida, K. Minomo, and K. Ogata, *Phys. Rev. C* **94**, 044604 (2016).
- [28] A. Tohsaki, H. Horiuchi, P. Schuck, and G. Röpke, *Phys. Rev. Lett.* **87**, 192501 (2001).
- [29] Y. Funaki, H. Horiuchi, A. Tohsaki, P. Schuck, and G. Röpke, *Prog. Theor. Phys.* **108**, 297 (2002).
- [30] B. Zhou, Y. Funaki, H. Horiuchi, Z. Ren, G. Röpke, P. Schuck, A. Tohsaki, C. Xu, and T. Yamada, *Phys. Rev. Lett.* **110**, 262501 (2013).
- [31] B. Zhou, Z. Ren, C. Xu, Y. Funaki, T. Yamada, A. Tohsaki, H. Horiuchi, P. Schuck, and G. Röpke, *Phys. Rev. C* **86**, 014301 (2012).
- [32] Y. Funaki, A. Tohsaki, H. Horiuchi, P. Schuck, and G. Röpke, *Phys. Rev. C* **67**, 051306(R) (2003).
- [33] Y. Funaki, A. Tohsaki, H. Horiuchi, P. Schuck, and G. Röpke, *Eur. Phys. J. A* **24**, 321 (2005).
- [34] Y. Funaki, H. Horiuchi, W. von Oertzen, G. Röpke, P. Schuck, A. Tohsaki, and T. Yamada, *Phys. Rev. C* **80**, 064326 (2009).
- [35] B. Zhou, Y. Funaki, H. Horiuchi, Z. Ren, G. Röpke, P. Schuck, A. Tohsaki, C. Xu, and T. Yamada, *Phys. Rev. C* **89**, 034319 (2014).
- [36] M. Lyu, Z. Ren, B. Zhou, Y. Funaki, H. Horiuchi, G. Röpke, P. Schuck, A. Tohsaki, C. Xu, and T. Yamada, *Phys. Rev. C* **91**, 014313 (2015).
- [37] M. Lyu, Z. Ren, H. Horiuchi, B. Zhou, Y. Funaki, G. Röpke, P. Schuck, A. Tohsaki, C. Xu, and T. Yamada, [arXiv:1706.06538](https://arxiv.org/abs/1706.06538).
- [38] P. Ring and P. Schuck, *The Nuclear Many-Body Problem* (Springer-Verlag, New York, 1980), p. 474.
- [39] A. B. Volkov, *Nucl. Phys.* **74**, 33 (1965).
- [40] N. Yamaguchi, T. Kasahara, S. Nagata, and Y. Akaishi, *Prog. Theor. Phys.* **62**, 1018 (1979).
- [41] S. Okabe and Y. Abe, *Prog. Theor. Phys.* **61**, 1049 (1979).
- [42] N. Itagaki and S. Okabe, *Phys. Rev. C* **61**, 044306 (2000).
- [43] T. Suhara and Y. Kanada-En'yo, *Prog. Theor. Phys.* **123**, 303 (2010).
- [44] F. Kobayashi and Y. Kanada-En'yo, *Phys. Rev. C* **86**, 064303 (2012).
- [45] D. R. Tilley, J. H. Kelley, J. L. Godwin, D. J. Millener, J. E. Purcell, C. G. Sheu, and H. R. Weller, *Nucl. Phys. A* **745**, 155 (2004).
- [46] G. Audi, F. G. Kondev, M. Wang, B. Pfeiffer, X. Sun, J. Blachot, and M. MacCormick, *Chin. Phys. C* **36**, 1157 (2012).
- [47] H. Morita and Y. Kanada-En'yo, *Phys. Rev. C* **96**, 044318 (2017).